

An Inventive High-Thrust Micro-Propulsion System Compatible with Small-Satellites' Safety and Budget Requirements

Executive Summary Report (ESR) Early Technology Development

Open Space Innovation Platform (OSIP) Discovery Channel
"IDEA: I-2022-05117"

**Affiliation(s): Sirin Orbital Systems AG (Prime, CH),
Zürich University of Applied Sciences ZHAW (Sub, CH)**

Activity summary:

The need for high-thrust propulsion systems compatible with small satellites for constellation deployment, orbit maintenance and stationkeeping is particularly emerging. A high-thrust propulsion system provides large velocity increments in a short time, which enables orbit transfer, orbital plane change, re-entry, and planetary orbit insertion for deep space exploration. In this activity, we developed the concept of water vapor and metal powder pulsed-micropropulsion system, with advantageous features: (i) safe, non-toxic/ hazardous propellant, (ii) high-thrust despite compact footprint, (iii) in-space availability of propellants.

→ THE EUROPEAN SPACE AGENCY

Publishing Date: **04.07.2024**
Contract Number: **4000141012**
Implemented as ESA EXPRESS PROCUREMENT – EXPRO

ESA Discovery & Preparation
From breakthrough ideas to mission feasibility. Discovery & Preparation is
laying the groundwork for the future of space in Europe
Learn more on www.esa.int/discovery
Deliverables published on <https://nebula.esa.int>

An Inertive High-Thrust Micro-Propulsion System Compatible with Small-Satellites' Safety and Budget Requirements

Masaya Murohara^{a,b}, Marius Banica^a, Madi Matteo^b

^a *Institute of Energy Systems and Fluid-Engineering, Zurich University of Applied Sciences, Technikumstrasse 9, 8401 Winterthur, Switzerland*

^b *Sirin Orbital Systems AG, Genferstrasse 24, 8002 Zürich, Switzerland. contact@sirin-os.com*

Abstract

This activity is to improve technology level of innovative micro-propulsion system for small satellites. This system uses a combination of water vapor and metal powder (Al/Mg) as propellants to achieve high thrust. The activity mainly composed of three work packages (WPs). In WP1, metal powder supply system was developed and pulsed powder supply was demonstrated. In WP2, water vapor and aluminium powder combustion was demonstrated. By the combustion test, it was clarified that the ejected particles from nozzle were mostly smaller than 100 μm , and the estimated performance by the combustion were thrusts of 204.9 mN and specific impulses of 118.6-206.5 s. In WP3, assessment of scalability and competitiveness in market were done.

Acronyms/Abbreviations

BBM	:	Bread Board Model
CCN	:	Combustion Chamber and Nozzle
CCP	:	Condensed Combustion Particle
COTS	:	Commercial-off-The Shelf
GEO	:	Geostationary Orbit
LEO	:	Low Earth Orbit
MPSS	:	Metal Powder Supply System
PSD	:	Particle Size Distribution
R&D	:	Research and Development

1. Introduction

Small satellites have become the backbone of the new space infrastructure and have proven their usefulness and importance for education, technology demonstration, telecommunications, Earth observation, and more [1,2]. To further expand small satellite activities, micro-propulsion systems are needed. A micro-propulsion system cannot be developed by a simple scale-down of "conventional" propulsion systems due to its strict constraints with regard to safety, cost, mass, volume, and power. Hence, micro-propulsion systems are often unique, which renders the associated research and development a very active and innovative field, involving many universities and companies.

R&D for cold-gas thrusters and electrical propulsion has seen significant progress, but that of chemical micro-propulsion is somewhat delayed, which might be linked to its inherent dangers. Because chemical micro-propulsion can generate high thrust offering the capabilities of rapid orbit transfers, planetary orbit insertions, asteroid flybys, and controlled re-entries, the development of a chemical propulsion system compatible with safety requirements, cost, mass, volume, and power restrictions of small satellites is urgently needed, given the emerging needs of the New Space market.

Due to environmental restrictions, several micro-propulsion system candidates use green propellants,

which have high safety, density, and stability. Representatives of this class include ADN/HAN-based propellants. ADN-based propellants were demonstrated in orbit, and achieved thrust levels within the range 0.1-1.0 N with a specific impulse of ≈ 220 s [3]. While this propellant has many advantages, it also has significant disadvantages for the use in micropropulsion systems: 1) its generation and handling require chemical knowledge, and its acquisition route is limited for the private sector; 2) for the combustion, it requires platinum catalysts, which increase the development costs and lead-time; 3) it requires pre-heating up to approximately 600 K, which decreases energetic efficiency and increases time to availability [4,5]; 4) it requires the installation of secondary propellant/propulsion system to achieve precise orbit/attitude control.

Water and metal powder based micropropulsion has the potential to solve these issues since: 1) the handling of water and aluminium powder does not require specialist knowledge, certification, or equipment, and commercial-off-the-shelf (COTS) materials can be used; 2) for the ignition, any igniter will work, and pre-heating up to ~ 400 K is sufficient; 3) by feeding water via other lines, the water and metal powder micro-propulsion system can be expanded to become a multimode micro-propulsion system with a water resistojet thruster and a gridded-ion or hall-effect thruster [6-9]. For example, the water resistojet thruster "AQUARIUS" (thrust level is ~ 4 mN) was developed and operated by one of the current team members and achieved in-orbit demonstration [8,9].

Adding to the above advantages, the proposed propulsion system is expected to show significant potential in the future: 1) once the multimode-propulsion is achieved, small satellites will be able to achieve more challenging missions [6]; 2) water and aluminium exist on the Moon, and there is a possibility of in-situ resource utilization [10]. 3) the ultimately safe and low-cost

propellants (water and aluminium) will lower the hurdles for private companies/universities to enter satellite development. These advantages are fascinating even if its propulsive performance is lower than that of ADN/HAN-based propellants.

Based on the background above, we propose a chemical micropropulsion using the combustion of water vapor and metal powder. A schematic of the proposed system is shown in Figure 1. The water and metal powder are stored in separate tanks. The water is supplied to the vaporizer by a blow-down system and evaporated there. The water vapor is also supplied to the combustion chamber by blow-down system. On the other hand, the metal powder is supplied to the combustion chamber by a carrier gas that is a part of the pushing gas stored in the water tank. The two propellants are ignited by a spark, and combustion gas and combustion condensed particles (CCPs) are exhausted through the nozzle. The gas is accelerated in nozzle and is expected to generate 0.1-1 N thrust. The key point of this system is that it applies pulsed-firing operation. This means that the propellant supply is stopped when the combustion chamber pressure is higher than the propellant tank pressure. Pulsed operation can decrease the system pressure keeping propulsive performance [11,12]. The concept itself is simple, but it has some fundamental challenges that need to be studied: 1) the need for an adequate metal powder supply system (MPSS) and 2) the possibility of generating excessive CCP sizes, which would produce space debris.

Generally, MPSS are classified into two types: mechanical supply systems and carrier gas supply systems [13]. Mechanical supply systems have mechanical moving parts, such as rotary or screw gears, to transfer powder from a tank to a target location. However, the moving parts make the system complicated and result in an increase of system mass, volume, and a malfunctioning risk. Carrier gas supply systems, on the other hand, are very simple in design. Typical powder supply systems intended for use in space integrate both types. They have a screw jack, which is not used for powder supply, but rather to regulate the distance between the powder bed surface and a carrier gas inlet. Bell Aerospace company developed a powder supply system in the 1960s and early 1970s. However, it should be noted that such systems require seals between the powder tank and the screw jack to prevent powder from entering the latter. This sealing system may be a cause of malfunction. Therefore, a carrier gas supply system without any mechanical transport means is desirable.

In 2009, Ogata reported on the development of a carrier gas supply system without any mechanical transport means [14]. Since the reported system is for continuous powder supply, the pulsed supply characteristics are not clarified.

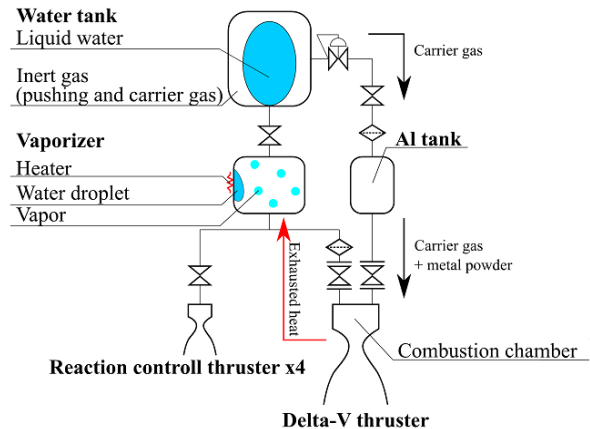


Figure 1 Schematic of proposed water and metal-powder micro-propulsion system.

CCPs have negative effects on the space environment. If the size of the ejected CCPs is larger than 1 mm, the particles will be determined space-debris, and the propulsion system will not be allowed to operate in LEO/ GEO [15] regardless its propulsive performances. However, in order to limit possible orbit contamination, it is perhaps reasonable to strive for CCPs sizes that are significantly smaller than 1 mm, say, by a factor of ten. Therefore, clarifying the CCP particle size distribution (PSD) is a key factor for the appropriate assessment of the present propulsion system. CCPs might also have negative impacts on the thruster itself. For example, CCP agglomeration in the nozzle throat area carries with nozzle throat clogging risks. This would result in the failure of the propulsion system.

The present activity aimed at solving these issues or clarifying the negative impacts described above. The main topics were the development of the MPSS and the combustion chamber and nozzle (CCN). We designed and constructed breadboard models (BBMs) for both, and successfully demonstrated pulsed powder supply, as well as water vapor and metal powder combustion. The objectives of the MPSS development were 1) investigation and evaluation of techniques to store the metal powder and distribute it to the combustion chamber in a consistent and controlled manner under 1G conditions; 2) to maintain a constant powder mass flow rate or a prescribed powder mass flow rate as a function of time under 1G conditions, 3) to determine the system power requirements. The objectives of the CCN development were 1) the characterization of CCPs injection rates and PSDs; 2) the investigation of CCP built-up in the nozzle throat area; 3) the measurement and control of thrust, specific impulse, combustion efficiency, and power requirements. In addition to that, we carried out a market survey and an assessed the competitiveness of our product based on the current experimental results. Finally, we reviewed potential contamination issues due

Table 1 The test conditions for MPSS demonstrator.

Test. #	Carrier gas pressure [kPaG]	Carrier gas mass flow rate, [mg/s]	Storage tank diameter [mm]	Filling rate	Open/close frequency [Hz]	Open time [ms]
#01	100	~15	23	0.3	0.25	100
#02	100	~15	23	0.3	0.50	100
#03	100	~15	23	0.4	0.25	100
#04	100	~30	23	0.3	0.25	100

to the presence of CCPs in electromagnetic fields and evaluated the scalability of the proposed system.

2. Methods

2.1 WP1: MPSS

Figure 2 and Figure 3 show a schematic of and the physical system of the MPSS, respectively. The system uses compressed air as a carrier gas to fluidize the metal powder in the powder tank and supply it to the downstream components. In a full propulsion system, the latter would mainly consist of the combustion chamber. However, for the MPSS demonstrator, we used a powder collector tank as a substitute. The gas-powder mixture flow is regulated by the pinch-valve which is shown in Figure 4. The valve is composed of an actuator and springs and is normally closed. When in this position, the power is turned off, and the valve closes a powder line by pinching it with the aid of a plunger and loaded springs. When a current is applied to the actuator, it pulls the plunger against the springs to open the line, and the powder-carrier gas mixture can flow through the valve.

We successfully demonstrated MPSS operation by measuring the ejected powder mass into the collector tank in each shot. The carrier gas pressure and valve opening time were set as constant, 200 kPa and 100 ms, respectively. The parameters were carrier gas mass flow rate, filling rate, and open-close frequency. The conditions are listed in Table 1. The filling rate was determined by powder mass per powder bed volume.

2.2 WP2: CCN

A schematic of the CCN test rig and the physical model are shown in Figure 5. The water vapor supply line and CCN are covered by heaters and heated up to over 100 °C to prevent condensation. Windows for optical access are built into both the combustion chamber and the vacuum chamber and are heated by heat guns to minimize the risk of condensation. The combustion chamber is of rectangular shape, with width 50 mm, depth 50 mm, and height 100 mm. The nozzle throat diameter is 1 mm. The CCN has a volume of approximately $3 \times 10^{-4} \text{ m}^3$. The oxidizer mass in the CCN is a function of chamber pressure. The combustion chamber pressure settles to an equilibrium value when the water vapor inlet mass flow rate equals its outlet mass

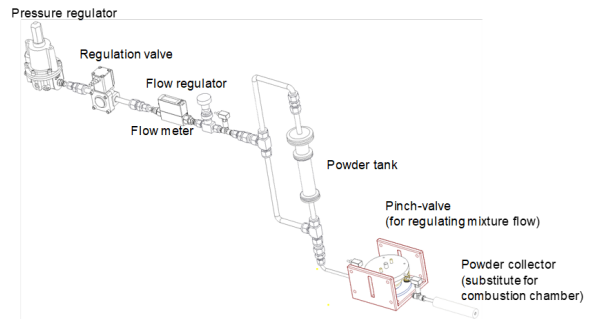


Figure 2 MPSS schematic.

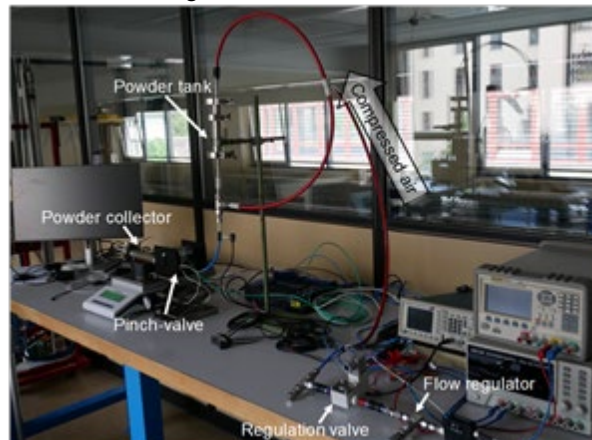


Figure 3 Physical MPSS built for the project.

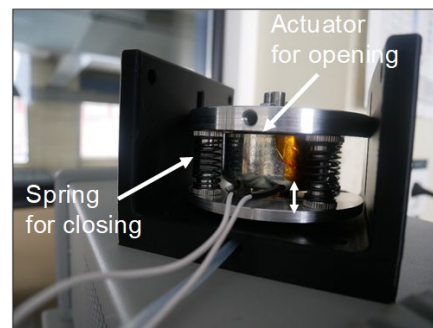


Figure 4 Powder valve for the control of the powder supply.

flow rate through the nozzle throat. The aluminium powder was supplied to the combustion chamber with the MPSS. The supplied water vapor and metal powder were ignited by an AC igniter with an output voltage of 12

Table 2 Investigated aluminum powder characteristics

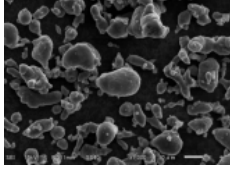
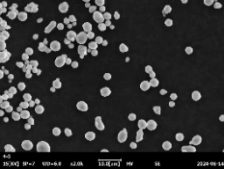
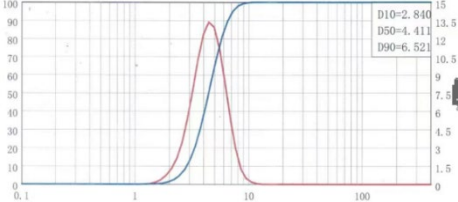
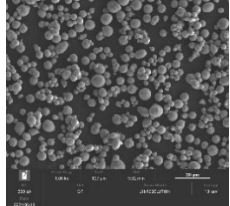
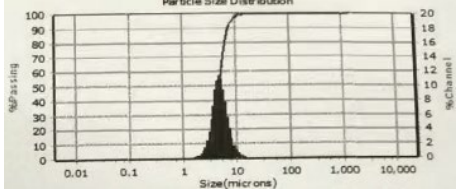
No.	Supplier (Country)	Size, μm	Shape*	Size distribution*
#01	Toyal Europe (FR)	4.2 \pm 1.3		$d_{10} = 2.2 \mu\text{m}$ $d_{50} = 4.2 \mu\text{m}$ $d_{90} = 7.8 \mu\text{m}$
#02	Stanford Advanced Material (US)	4.4 \pm 0.8		
#03	Vi Halbleitermaterial (DE)	4.9 \pm 3.1		

Table 3 Experimental conditions

Exp. No.	Powder No.*	H ₂ O mass (pressure)	Injected powder mass	Ox./Fu. ratio
#01	#01	143.7 mg (80.4 kPa)	308.3 \pm 37.8 mg	0.47 \pm 0.06
#02	#02	129.1 mg (71.6 kPa)	201.7 \pm 75.6 mg	0.64 \pm 0.25
#03	#02	117.0 mg (64.4 kPa)	563.6 \pm 112.6 mg	0.21 \pm 0.04
#04	#03	134.3 mg (74.7 kPa)	-	-

* Powder #01: from Toyal Europe (FR), Powder #2: from Stanford Advanced Material (US), and Powder #03: from Vi Halbleitermaterial.

kVAC and electric current of 55 mA. The combustion generated combustion gas and CCPs. The CCPs were ejected through the nozzle and observed by means of a high-speed camera. A laser sheet was introduced to generate a clear focal plane and illuminate both unburned and burned powders. This allowed the collection PSD data through adequate post-processing.

We obtained 170 images in total per experimental run with a shooting frequency of 14 fps. This shooting frequency was limited by the charging time of the laser. The PSDs were analysed by processing the images with an in-house code. The processing procedure was carried out in five steps by 1) setting the upper limit of sensitivity of the camera to avoid noise, 2) binarizing the image with Otsu's method, 3) morphological processing to remove noise, 4) detecting contours of particles, and 5) calculating particle diameters.

We prepared three types of aluminium powders from different suppliers to see the impact of shape and powder PSD on the CCP PSDs. These powders were purchased from Toyal Europe (France), Stanford Advanced Material (USA), and Vi Halbleitermaterial (Germany).

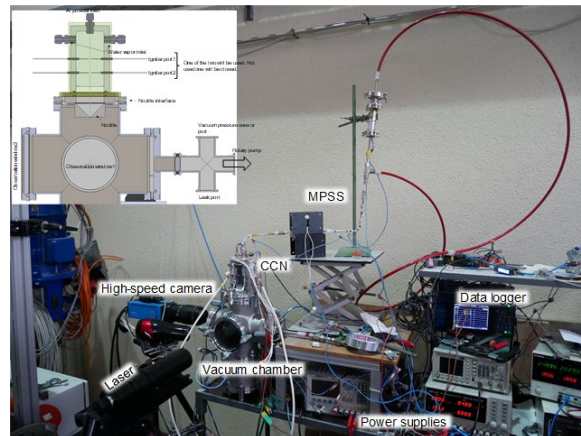


Figure 5 The appearance of the test rig. The CAD image in upper left is the enlarged view of CCN and vacuum chamber.

Their characteristics are shown in Table 2, and the experimental conditions are shown in Table 3. The injected powder mass and mixture ratio of powder #03 (from Vi Halbleitermaterial) are unavailable because the

powder supplying was failed in the injected powder mass measurement.

2.3. WP2 & WP3: Performance estimation and assessment of competitiveness

Key performance parameters such as thrust, specific impulse, combustion efficiency, and power requirements, were estimated based on the experimental results. The thrust and specific impulse were estimated with an assumed specific heat ratio for the gas, assumed temperature, and measured pressure. The combustion efficiency was estimated from a comparison between the measured and ideal combustion pressure. The ideal combustion pressure was calculated by NASA's Chemical Equilibrium with Applications (CEA) software [16]. The input for the ideal calculation was ignition pressure, injected powder mass and temperature. The injected powder mass and pressure were measured by us, and temperature were assumed minimum and maximum number. The minimum temperature was assumed to be the same temperature of water vapor temperature when ignition, and the maximum temperature was assumed to be ideal, i.e., the calculated temperature by NASA's CEA. The power requirement was evaluated by the power consumptions by powder valve, igniter, and water supply. Power input for the water supply is required to ready the propulsion system for ignition, but, in a matured system, after several pulsed firings, heating could cease since regenerative heat from the combustion chamber could be used instead. However, the initial heating power accounts for the majority of the (peak) power requirements.

The estimated performance measures were compared with those of other micro-propulsion systems. Most of the data on competitors was collected from a report provided by NASA [17]. We plotted two maps; thrust vs. specific impulse, and total impulse vs. propulsion system size. In addition to that, we estimated propulsion system mass and size for various commercial satellites under the assumption that the present propulsion system is installed in these as a replacement for existing systems.

3. Results

3.1. WP1: Injected powder mass and power consumption

We demonstrated the MPSS by measuring the ejected powder mass in each shot under the conditions shown in Table 1. For each test case, ten consecutive injections were demonstrated, and the average ejected powder masses per injection are shown in Figure 1.4 for the various test cases. The test number #3 shows the injected powder mass of 0 mg. We believe that this was because the powder in the powder tank was not fluidized well due to the filling rate, which was higher than for the other three test cases. In the three successful tests, #1, #2, and #4, we demonstrated the efficacy of the powder supply and obtained injected powder masses of 930-1'140

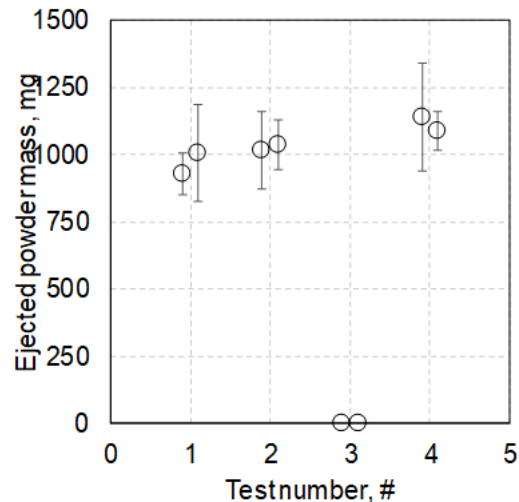


Figure 6 Ejected powder mass for each test number. The test number is indicated on the horizontal axis (cf. Table 1).

mg/shot depending on the condition. Also, the powder supply showed good repeatability. The variations of the injected mass were in the range of 0.1-18.5% against the average injected powder mass in each test. The supplied powder to carrier gas mass ratio was in the range of 294.9-413.8. Thus, we can conclude that the amount of carrier gas mass is too small to affect the combustion.

The power consumption of the MPSS solely depends on the operation time of the actuator. The required voltage and current were ~28 V and ~5 A, respectively, and it was opened during 100 ms in every 4 s in the experiments. This means that the time-averaged consumed power was 3.5 W. This power supply level is feasible even for micro-satellites. The flight model that will be built in the future will have higher actuation frequencies, for instance 1 Hz. Even with this frequency, however, the power consumption will be approximately 14 W based on the current assessments, but might be reduced further depending on the design evolution of the pinch valve.

3.2. WP2: Ejected CCPs size distribution

The CCP PSDs were as shown in Figure 7. The result shows that more than 99.9% of ejected CCPs (including non-reacted particles) were smaller than 100 μm regardless of the type of powder used. Furthermore, the results of experiments No. #01, #02 and #04, imply that the differences in shape (non-spherical or spherical), did not have a significant impact on the PSDs. A comparison between experiments No. #02 and #03 shows that the mixture ratio did not have a significant impact on the PSDs either. The mode value of the PSD was ~50 μm in all experiments even though the powder particle sizes were smaller than 10 μm (see Table 2). This result implies that the CCP PSD depends on the powder PSD, and that the powders experienced agglomeration.

3.3. WP2: Accumulation of CCPs in nozzle

The retained particle mass in the nozzle was measured in experiments No. #02 and #03. The accumulated powders, shown in Figure 8, did not clog the nozzle throat. This was also indicated by the fact that CCPs continued to be ejected from the nozzle after each injection. The powder did also not stick to the CCN walls. When the nozzle was flipped, the powder fell off smoothly. This fact implies that the nozzle throat diameter of 1 mm was too small to exhaust the powder.

The accumulation of CCPs was quantified by calculating the mass fraction between retained and total injected powder. In experiments No #02 and #03, 27% and 49% of the injected powder was retained, respectively. The two results implied that the larger injected powder mass resulted in a larger retained powder mass fraction. Therefore, we should consider a trade-off between the propulsive performance and powder accumulation, which is important for the lifespan of the propulsion system. Nozzle optimization and minimization of retained powder mass fractions will be addresses a follow-on project.

3.4. WP2: Combustion pressure and performance estimation

The pressure time histories for each experimental run are shown in Figure 9. In experiments #02, #03, and #04, some pressure increase can be observed even without the powder injections, for instance, at $t \approx 10$ s and $t \approx 16$ s in #02. We believe that these pressure increases are not physical, but rather result from electrical noise due to the ignition spark. In experiment #01, the powder was not injected during the first and second powder valve actuation. The first powder injection occurred in the third valve actuation, and the powder combusted. In the following injections, we observed combustion events that were accompanied by bright flashes from the combustion chamber, but the pressure did not increase to the extent it did during the first combustion event. In contrast, three continuous pulsed pressure increase can be seen in the experiment #01. The difference between the two experiments was the injected powder mass.

From Figure 9, it is clear that the pressure increase ratio in experiment #03 was higher than in the other three experiments. The difference between the experimental runs was in the injected powder mass. This fact implies that higher injected power mass is important for higher combustion pressure. It should be noted that we cannot say whether the powder mass of interparticle distance is more important.

The thrust and specific impulse were estimated with an in-house code. The estimation assumed 1) the flow was quasi one-dimensional, 2) the flow was frozen, and 3) the exhausted gas was water vapor only. The third

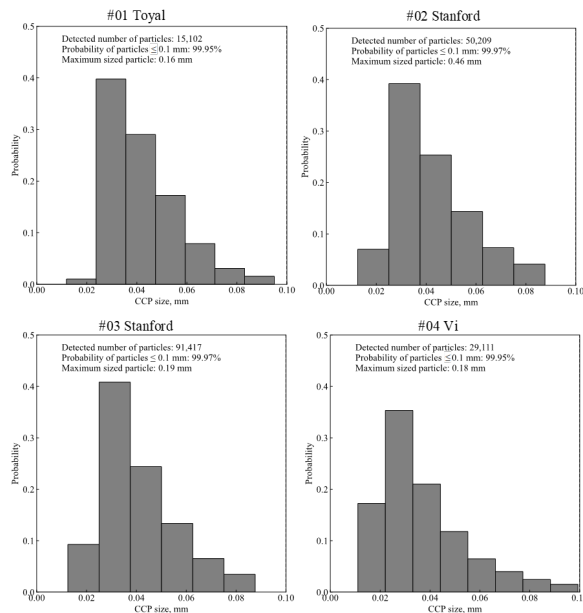


Figure 7 Experimental result of CCPs size distribution.

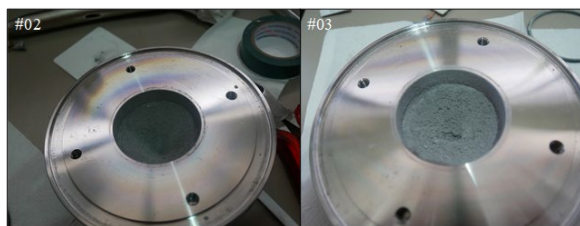


Figure 8 Accumulated powder in nozzle after each experimental run.

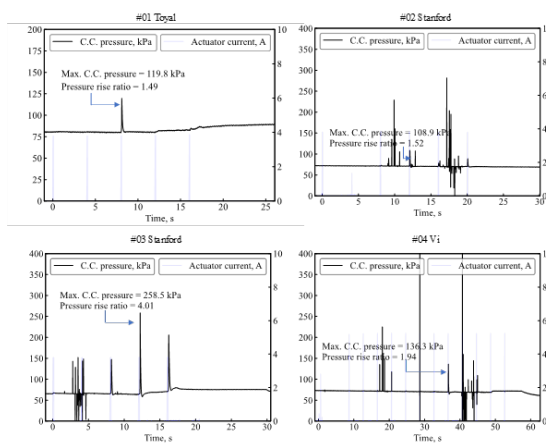


Figure 9 Pressure time history of each experimental run. The time $t = 0$ indicates the time of the first powder valve operation.

assumption was deduced from the output of a CEA calculation. This output showed that the mass fraction of condensed-phased aluminium and aluminium oxide was approximately 94% among all generated elements. This assumption led to a lower estimation since the

combustion gas specific heat ratio must be lower than that of water vapor, and smaller specific heat ratio in general leads to higher thrust and specific impulse. Our estimates for thrust and specific impulse are, therefore, conservative.

Using the measured data of experiment #02, a thrust of 204.9 mN and a specific impulse of 118.6-206.6 s were achieved. It should be noted that the specific impulse did not take the residual powder mass in the combustion chamber into account, and that thrust is only generated during combustion.

3.5. WP3: Potential hazard by CCPs

The proposed micropropulsion system exhausts CCPs from its nozzle. Qualitatively, there is a concern that charged CCPs are captured by the Earth's magnetic field, and the CCPs are recirculated back to the satellite where they might impact and cause damage to optical or telecommunication equipment. To assess the plausibility of this hypothesis, we evaluated the Larmor radius for the CCPs. Assuming that the particle velocity is 1 m/s and the electrical charge is 1 $\mu\text{C}/\text{kg}$ [18] (this is an order estimate), the Larmor radius was evaluated as shown in Figure 10 and found to be in the order 10^{10} m, which is large enough to deduce that the possibility of CCPs impacting on the satellite due to the Earth's magnetic field is negligible. Due to the large value of the Larmor radius, this should still hold for velocities and electrical charges that are orders of magnitude higher than what we have assumed here.

3.6. WP3: Assessment of scalability

We assessed the geometrical and thrust scaling limitations. For the geometrical scaling, we considered lower and upper limit of combustion chamber diameter, length, volume, and nozzle throat diameter. The combustion chamber diameter and length are limited by the quenching distance of the chemical reaction. The quenching distance of micron-sized aluminium powder in water vapor is unknown, but that in air was reported by Goroshin et al. [19]. The distance is ~ 20 mm, so the combustion chamber diameter and length must be larger than 20 mm. On the other hand, the diameter and length have no upper limitation related to physical phenomena. Rather, the upper limit will be determined by the installation space on the satellite.

The lower limit for the combustion chamber volume is determined by the minimum suppliable powder mass. The powder mass flow rate obtained in WP1 was as shown in Figure 11. It shows that the minimum powder mass flow rate was approximately 4'400 mg/s since the minimum fluidization carrier gas mass flow rate was ~ 1 mg/s. Assuming that the shortest powder injection time is 60 ms, which is based on the response speed of the pinch-valve developed in WP1, the minimum suppliable

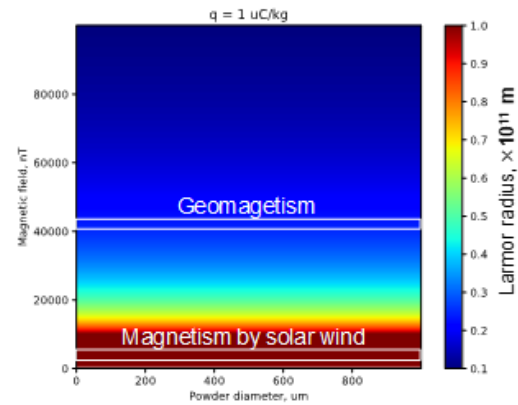


Figure 10 Larmor radius map with parameters of magnetic field and powder diameter.

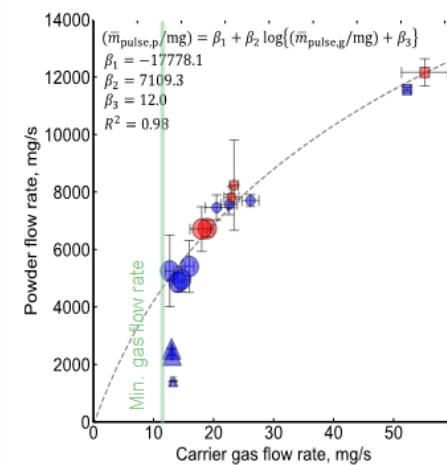


Figure 11 Powder flow rate vs. carrier gas flow rate from the result of WP1.

powder mass is calculated from $4'400 \text{ mg/s} \times 60 \text{ ms/shot} = 264 \text{ mg/shot}$. Since the oxidizer mass depends on the combustion chamber volume if we assume the combustion chamber pressure as 100 kPa, the relation between the combustion chamber volume and the mixture ratio can be obtained. Assuming a mixture ratio of 0.21, which is based on the result of WP2.4, the minimum combustion chamber volume is ~ 0.1 U. The optimal mixture ratio will be explored in a future project.

The upper limit of the combustion chamber volume is determined by the required filling time of the water vapor when the nozzle throat diameter is selected. This means that there is no upper limitation stemming from physical considerations. Rather, the limitations are linked to technical assessments, since larger combustion chamber volumes requires larger mass flow rates for the propellants. The flow conductance, which is a typical number used to evaluate the mass flow rate in hydraulic networks, has the biggest impact on the filling time. The

filling time is as shown in Figure 12. The conductance $C = 1 \times 10^{-8} \text{ kg}/(\text{Pa s})$ is a number used in a water resistojet thruster AQUARIUS which is a propulsion system of 6U CubeSat EQUULEUS[20]. Since the combustion time was in the range of 0.1 second-level from the result of WP2, the filling time has to be much shorter than that or the time-averaged thrust becomes smaller. Therefore, the upper limit of the combustion chamber would be approximately 0.1 U for a target ignition pressure of 95 kPa. If we can prepare a valve having higher flow conductance, for instance $C = 10 \times 10^{-8} \text{ kg}/(\text{Pa s})$, the upper limit would be approximately 1.5 U.

The nozzle throat diameter must be large enough not to prevent the powders exhaustion. From the result of WP2, the diameter should be larger than 1 mm. On the other hand, the upper limitation of the diameter is determined by the power consumption required to ready the system for ignition. For this, water vapor must be generated and supplied to the combustion chamber until the ignition pressure is reached. The power is mainly used to compensate the latent heat of water (i.e. to evaporate the liquid). So, the required power for the water vapor supply is proportional to the mass flow rate at the nozzle throat, and the mass flow rate is proportional to the nozzle throat area. Thus, we can estimate the power consumption as shown in Figure 13. When the nozzle throat diameter is designed larger for preventing the accumulation of powder at the nozzle, the required power for water vapor supplying becomes larger or the achieved ignition pressure becomes lower because the outlet mass flow rate of water vapor becomes larger. Therefore, there will be a trade-off between the power required to ready the system for ignition, and the accumulation of powder at the nozzle. Figure 13 shows that when the ignition pressure is set as ~60 kPa, about 1 kW is required for the initiation. This power is unrealistically large for CubeSats, but 300 kg sized satellites can afford it.

The thrust is proportional to the mass flow rate, the mass flow rate proportional to the nozzle throat area, and hence to the throat diameter squared. As a result, the thrust is also proportional to the nozzle throat area assuming that the combustion characteristics such as combustion pressure, gas composition, and gas temperature, are independent from nozzle throat diameter. Thrust can be scaled to for instance ~2 N with power input of ~1 kW for initiating the operation. This power input is required only for the first several pulses, and later, the system can use regenerative heat taking advantage of the heat loss from the combustion.

3.7. WP3: Assessment of competitiveness in market

In Figure 14, various commercial propulsion systems are shown. The different technologies are represented by the symbol colours. The data is collected from a report published by NASA[17]. The current propulsion system is represented by two rhombi, one for the currently

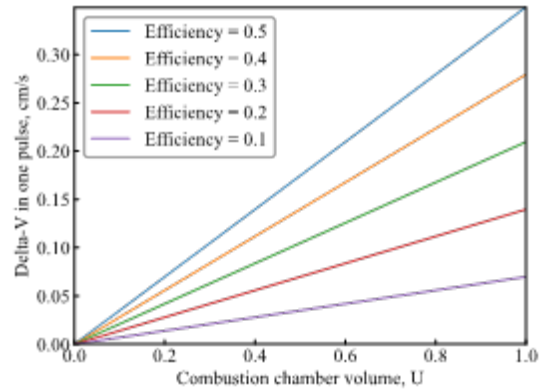


Figure 12 Relation of combustion chamber volume and delta-V in one pulsed firing.

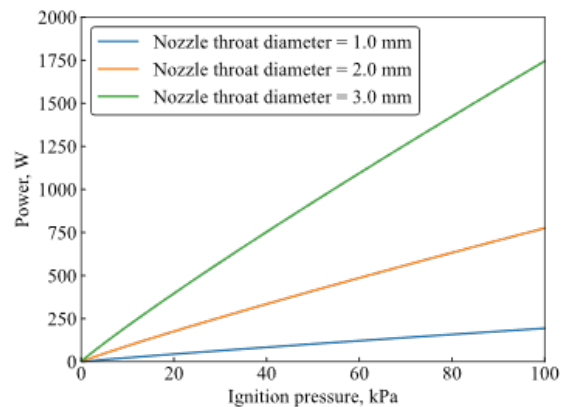


Figure 13 Required power for initiating the micropropulsion system against an ignition pressure.

expected best case (BC) and one for the currently expected worst case (WC).

Figure 15 shows the total impulse of various of the commercially available propulsion systems as a function of system size. Also shown is the propulsion system proposed here. The best and worst case are marked again by two rhombi. These are based on the currently obtained combustion efficiencies. The combustion efficiencies will be increased in follow-on work. As a result, we expect to either raise the total impulse for a given system size, or to reduce the system size for a given total impulse.

4. Conclusion

The need for high-thrust propulsion systems compatible with small satellites for applications such as constellation deployment, orbit maintenance and station-keeping is particularly emerging. We aim at the development of an innovative micro-propulsion system concept—patented by Sirin Orbital Systems AG (granted patent CH718280A2, priority: 2021-01-22, publication: 2022-07-29)—which uses a combination of water vapour and metal-powder (Al/Mg) as propellants to generate high thrust. The main differentiating advantages of the

targeted product are 1) safe, non-toxic and non-hazardous propellants, 2) high-thrust despite compact footprint, 3) in-space availability of propellants. This micro-propulsion technology will expand the mission field of small satellites and is applicable for both commercial and scientific missions. In this activity, we tackled three challenges to help further advance the technology, within three different work packages (WPs):

- WP1 development and demonstration of pulsed metal powder supply system including powder valve,
- WP2 demonstration of water vapor and metal powder combustion and confirmation of the size distribution of CCPs, and
- WP3 assessment of scalability and competitiveness in the current market.

Specifically, in WP1, we developed the MPSS, which is equipped with a pinch-type powder supply valve. The MPSS demonstrated continuous pulsed supply. The injected mass was in the range 930.0-1'140.0 mg/shot with variations of 18.5% or less. In addition, it was clarified that the injected powder mass can be controlled by the carrier gas pressure and mass flow rate. The prototype valve in MPSS was revised in WP2 to minimize electric power consumption. The final value obtained was ≈ 14 W.

In WP2, the CCN were built. Water vapor / aluminium powder combustion was demonstrated with it, and the generated and exhausted CCPs were observed with a high-speed camera and laser sheet to clarify the particle size distribution. For the experimental runs, three types of aluminium powders were prepared. The experimental runs clarified that most ejected CCPs were smaller than 100 μm in diameter, and that the powder shape (spherical or non-spherical) did not have a discernible impact on the size distribution. The injected powder mass also did not have impact on it, but it did affect the maximum combustion pressure. Large injected powder masses achieved thrusts of 204.9 mN and specific impulses of 118.6-206.5 s. Although activities in WP2 uncovered some additional challenges such as powder accumulation on the nozzle and destabilization of spark igniter after multiple combustion events, pulsed firing system was successfully demonstrated.

In WP3, three assessments were conducted: 1) of CCPs hazards for optical and telecommunication systems, 2) of system scalability, and 3) of system competitiveness in the current market. The assessment clarified that the hazards are extremely low. Also, the size limitations are mainly determined by the quenching distance of the powder, the minimum suppleable powder mass, and the water vapor supply time. The combustion chamber volume should be larger than 0.1 U, and the chamber diameter and length have to be 20 mm or longer. Based on the performance estimation and size scalability, we did a survey of the micropropulsion market and assessed

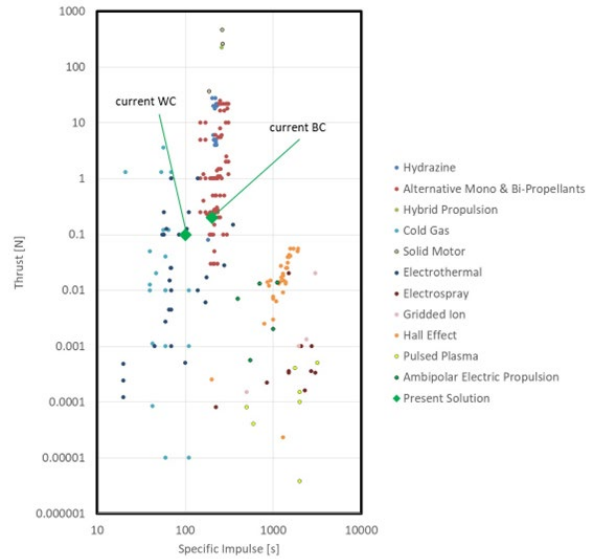


Figure 14 Thrust vs. specific impulse for the propulsion system. The present propulsion system is represented by the two green rhombi, which denote the current best case (BC) and the current worst case (WC) estimates.

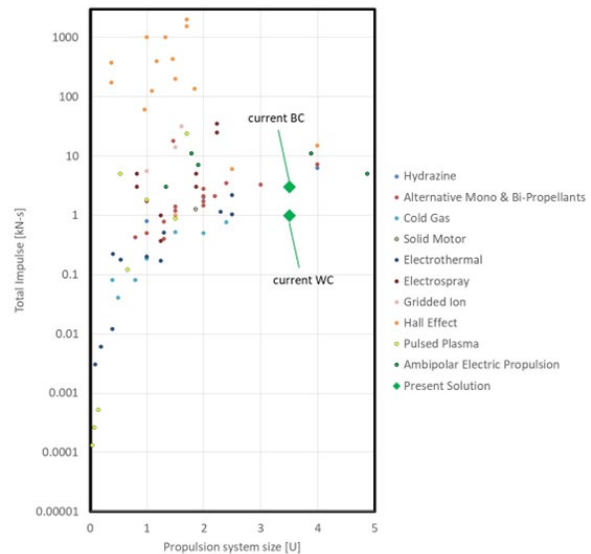


Figure 15 Total impulse vs. propulsion system size for propulsion systems given in. The present propulsion system is represented by the two green rhombi, which denote the current best case (BC) and the current worst case (WC) estimates.

the competitiveness of the proposed micropropulsion system. We found out that there is an excellent prospect for achieving comparable performance levels through future optimizations of our system. In addition, our micropropulsion system has many advantages other than performance, and we expect a market demand for this system once it is matured.

5. Reference

- [1] C. Williams, S. DePozzo, Nano-Microsatellite Market Forecast 10th Edition, Space Works, 2020. <https://doi.org/10.13140/RG.2.2.24280.32005>.
- [2] K. Lemmer, Propulsion for CubeSats, Acta Astronaut. 134 (2017) 231–243.
- [3] K. Anflo, R. Möllerberg, Flight demonstration of new thruster and green propellant technology on the PRISMA satellite, Acta Astronaut. 65 (2009) 1238–1249.
- [4] M. Negri, M. Wilhelm, H.K. Ciezki, Thermal ignition of ADN-based propellants, Propellants Explos. Pyrotech. 44 (2019) 1096–1106.
- [5] A.E.S. Nosseir, A. Cervone, A. Pasini, Modular Impulsive Green Monopropellant Propulsion System (MIMPS-G): For CubeSats in LEO and to the Moon, Aerospace 8 (2021) 1–26.
- [6] H. Koizumi, J. Asakawa, Y. Nakagawa, K. Nishii, Y. Takao, M. Nakano, R. Funase, Assessment of Micropropulsion System Unifying Water Ion Thrusters and Water Resistojet Thrusters, J. Spacecr. Rockets 56 (2019) 1400–1408.
- [7] J. Asakawa, H. Koizumi, K. Nishii, N. Takeda, M. Murohara, R. Funase, K. Komurasaki, Fundamental Ground Experiment of a Water Resistojet Propulsion System: AQUARIUS Installed on a 6U CubeSat: EQUULEUS, TRANSACTIONS OF THE JAPAN SOCIETY FOR AERONAUTICAL AND SPACE SCIENCES, AEROSPACE TECHNOLOGY JAPAN 16 (2018) 427–431.
- [8] Y. Ataka, Y. Nakagawa, H. Koizumi, K. Komurasaki, Improving the performance of a water ion thruster using biased electrodes, Acta Astronaut. 187 (2021) 133–140.
- [9] Y. Nakagawa, H. Koizumi, H. Kawahara, K. Komurasaki, Performance characterization of a miniature microwave discharge ion thruster operated with water, Acta Astronaut. 157 (2019) 294–299.
- [10] R.N. Clark, Detection of Adsorbed Water and Hydroxyl on the Moon, Science 326 (2009) 562–564.
- [11] P. Salgi, V. Balakotaiah, E. Ramé, B.J. Motil, Pulse properties in gas–liquid flow through randomly packed beds under microgravity conditions, Int. J. Multiphase Flow 73 (2015) 11–16.
- [12] A. Pasini, PulCheR- Pulsed Chemical Rocket with Green High Performance Propellant, 2016.
- [13] A.M. Ismail, B. Osborne, C. Welch, The potential of aluminium metal powder as a fuel for space propulsion systems, J. Br. Interplanet. Soc. 65 (2012) 61–70.
- [14] K. Ogata, Effect of Initial Void Fraction and Fluidized Air Flow on Spouting of Fine Powder through an Orifice, J. Soc. Powder Technol. 46 (2009) 187–196.
- [15] ESA Space Debris Mitigation Working Group, ESA Space Debris Mitigation Requirements, European Space Agency, 2023.
- [16] B.J. MacBride, S. Gordon, NASA Reference Publication 1311: Computer Program for Calculation of Complex Chemical Equilibrium Compositions and Applications II. Users Manual and Program Description, NASA, 1996.
- [17] Small Spacecraft Systems Virtual Institute, State-of-the-Art Small Spacecraft Technology, 2023.
- [18] 山隈瑞樹, 八島正明, アルミニウム粉投入中の粉じん爆発原因に関する実験的考察, 安全工学 50 (2011) 302–310.
- [19] S. Goroshin, M. Bidabadi, J.H.S. Lee, Quenching distance of laminar flame in aluminum dust clouds, Combust. Flame 105 (1996) 147–160.
- [20] K. Nishii, J. Asakawa, K. Kikuchi, M. Akiyama, Q. Wang, M. Murohara, Y. Ataka, H. Koizumi, R. Funase, K. Komurasaki, Flight Model Development and Ground Demonstration of Water Resistojet Propulsion System for CubeSats, Trans. Japan Soc. Aero. Space Sci. 63 (2020) 141–150.

– End of Document –